Innovative Coupling of PVT Collectors with Electric-Driven Heat Pumps for Sustainable Buildings

George Meramveliotakis[1], George Kosmadakis[1], Achileas Krikas[1], João Gomes[2,3] and Marika Pilou[1]

[1] Thermal Hydraulics and Multiphase Flow Laboratory, National Centre for Scientific Research "Demokritos", Agia Paraskevi (Greece)

[2] Department of Building Engineering, Energy Systems and Sustainability Science, University of Gävle, Gävle (Sweden)

[3] Research Department, MG Sustainable Engineering AB, Uppsala (Sweden)

Abstract

An innovative renewable-energy based system is examined for covering the heating and cooling demand in residential buildings. This system adopts an alternative solar-assisted heat pump configuration, developed around its two main components: the PVT collectors and a dual-source heat pump. The heat produced by the collectors can be either used directly for covering the heating needs or stored in a buffer tank for supplying the heat pump with low-temperature heat, exploiting all solar heat and operating the heat pump with an elevated performance for a longer period during the day. Once the stored heat in the buffer tank is discharged, the heat pump is supplied by ambient heat. The same configuration can also operate at cooling mode during summer, with the heat pump reversing its operation. The current work examines the main system parameters, in order to evaluate its performance for covering a large share of the building's energy needs.

Keywords: PVT collectors, dual-source heat pump, buildings, cooling and heating demand, domestic hot water

1. Introduction

Solar energy applications in buildings are increasing with many of them based on solar thermal collectors, photovoltaic (PV) panels or, in more advanced systems, hybrid photovoltaic-thermal (PVT) collectors (Buker and Riffat, 2016). At the same time, the use of domestic heat pumps for heating and cooling is rising (Guo and Goumba, 2018), because of their capacity to meet the buildings' energy demand, especially when they are supplied with low-temperature heat of up to 25 ^{o}C (Naranjo-Mendoza et al., 2019). The integration of the two above energy systems, i.e. solar-assisted heat pumps (SAHPs), results in maximum solar energy utilization and enhances the performance of the individual components, (Kim et al., 2018).

The main functionality of the integrated system is to either provide the required heat to the users directly from the solar collectors when the temperature is high enough or supply the heat pump with heat at low-temperature to increase its coefficient of performance (COP). A wide variety of thermal coupling methods exists, such as with direct or indirect heat transfer from the collector, aiming to improve the combined efficiency. Another concept that does not rely on the solar-assistance principal is the PV plus heat pump, which requires less piping and connections (Wang et al., 2020), with the main focus being placed on reducing the electricity consumption from the grid.

Based on the above general principles of combining either solar thermal collectors or PV panels with heat pumps, an alternative design is proposed here, based on the use of PVT collectors that produce simultaneously heat and electricity (Vaishak and Bhale, 2019). All the PVT heat production can be exploited in such coupling, even if it is at low-temperature and not used directly, but rather supplying the heat pump for greatly increasing its performance (Fine et al., 2017). The concept is realized here with:

- The use of standard water tanks to store either heating or cooling to cover the building energy demand,

doi:10.18086/eurosun.2020.05.01 Available at http://proceedings.ises.org

aiming to decouple to some extent the consumption from the production.

- The heat supply of the heat pump from either low-temperature water or ambient air, resulting to a dual-source unit, with the selection based on the maximum performance.

The integrated system is described in Section 2, where the main components and functions are presented, while the numerical model for its annual simulation based on typical building energy demand is presented in Section 3. Section 4 presents the main results of the system operation and performance during a winter and a summer day, as well as during a whole year for a multi-family residential building located in Athens (Greece). Finally, the conclusions of this study and the further steps are highlighted in Section 5.

2. System description

2.1 Overall layout

The main system components are the PVT collectors for producing heat and electricity and the dual-source (air or water) heat pump for heating and cooling. The system is intended for a multi-family residential building with the same concept also applicable in other types of buildings, such as single-family houses and offices after some modifications. The heating and cooling modes are illustrated in Fig. 1, along with the main system components and their connections.

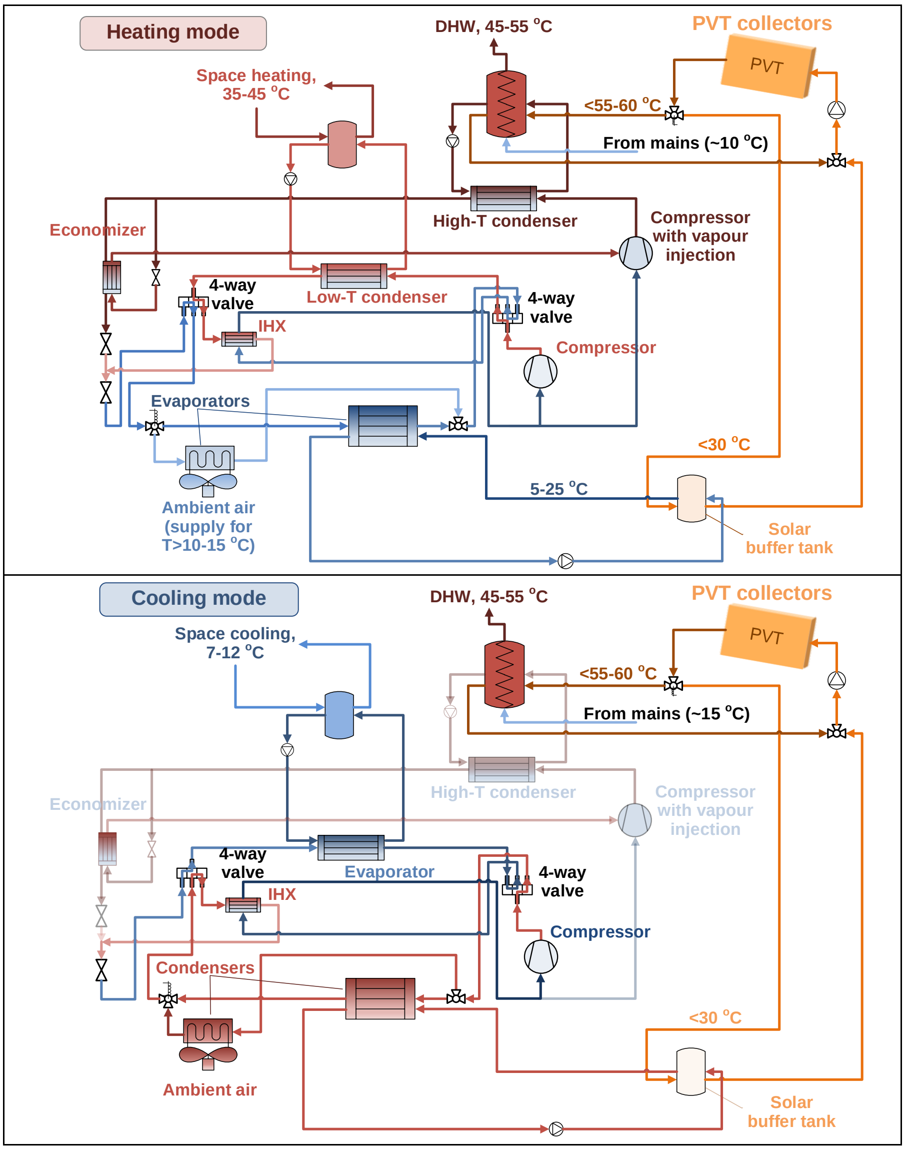

Fig. 1: System operation at heating mode (top) and at cooling mode (bottom), including the main system components

The electrical-driven heat pump is two-stage with the compressors placed in parallel. The high-temperature stage produces heat for domestic hot water (DHW) and is equipped with an economizer with vapour injection in the compressor. The low-temperature stage produces either space heating or space cooling and includes a subcooler (an internal heat exchanger – IHX) for increasing the COP. This configuration has been selected among many that have been examined (e.g. with in-series or parallel compressors, intercoolers, economizers) and showed the highest COP. Moreover, it can produce both heating and DHW at the same time.

For reversing the heat pump operation from heating to cooling mode and vice versa, two 4-way valves are included. One valve is the standard one placed at the compressor discharge, while the second one is necessary due to the presence of the subcooler at the outlet of the low-temperature condenser. The system operation for both the heating and cooling seasons is described next.

2.2 Heating season

For time intervals with adequate solar irradiation, the heat produced by the PVT collectors is of high enough temperature, over 45 °C, and charges the main water tank that is used for covering the building's domestic hot water (DHW) needs. Alternatively, when the solar radiation is low, the temperature of this heat is reduced and usually cannot be exploited by the main water tank. In the proposed system, this heat is stored in another tank (the "solar buffer tank") for supplying the evaporator of the heat pump and thus greatly increasing its COP to over 3.5-4 for DHW production at 55 °C (directed to the main tank) and space heating at 45 °C.

When the solar buffer is completely discharged and the temperature of the stored water drops below 5 °C, the heat pump switches its heat supply to ambient air. This flexibility is further enhanced with the presence of another buffer tank that stores the produced heat for the space heating needs, and decouples to some extent the time of heating demand with the heat pump operation, and thus reduce the electricity demand from the grid.

2.3 Cooling season

The system operation is simplified during the cooling season, since the heat produced by the PVT collectors is primarily stored in the main tank for covering the hot water needs of the building. At the same time, the solar buffer tank is always kept charged with a stored water temperature up to 25 °C, since usually there is an excess of solar heat production during summer. The purpose of storing heat also in the solar buffer tank is to allow a high heat pump performance for DHW production, in case the direct use of the collectors for charging the main water tank is not adequate. This is the case of a very high DHW demand.

However, the main function of the heat pump during the summer period is to deliver the space cooling at 7 °C, which is stored in the same buffer tank as space heating (heating is not used during this period). The reversing of the heat pump operation is necessary and no simultaneous production of DHW and space cooling is possible, always giving priority to the DHW. The effective cooling is provided in the evaporator, while the cycle rejects heat to the ambient through the air-cooled condenser.

3. Description of the numerical model

3.1 Overview

The complete system model has been developed in the Engineering Equation Solver – EES environment (Klein, 2020), and simulates the system operation during the average day of each month, using as input the energy demand, with the separate model of the latter described later. The system model is based on the modeling of its individual components, which are described next.

3.2 Heat pump

The two-stage heat pump uses a refrigerant with an ultra-low global warming potential (GWP). Two screened refrigerants have been examined that fulfill this, R1234yf and R1234ze(E), with the latter bringing a higher COP by up to 10-15% and a much higher heating capacity. Therefore, R1234ze(E) has been finally selected, with all simulations presented here relying on this HFO refrigerant.

As described previously, the heat pump has two separate condensers, one delivering heat for DHW production up to 55 ^oC and the other for space heating at 45 ^oC. At cooling mode, the cycle is reversed and only the low-temperature compressor operates rejecting heat to the ambient, as indicated in Fig. 1.

The heat pump modeling is based on a validated thermodynamic model developed in EES software (Kosmadakis and Neofytou, 2019), enriched to account for the finned-tube heat exchanger (HEX) and the compressor model, with the latter based on a semi-hermetic screw compressor of Bitzer with a displacement of 140 m^3/h at 50 Hz. The resulting heating capacity is 30 and 60 kW for DHW and space heating respectively.

Various simulation runs have been conducted leading to the sizing of the main components (e.g. the plate HEXs, air-fan). Once sizing was specified, the heat pump operation has been examined for variable heat source and sink temperatures. The results have been processed and used in a regression analysis for developing correlations of the key parameters, COP and heating/cooling production. These correlations are given as polynomials of the hot and cold side temperatures to allow a straightforward integration in the overall EES system model.

3.3 PVT collector

The PVT collector features an asymmetric low-concentration stationary reflector design, with a total size of 2.31 × 0.955 m. The thermal and electrical capacity is 1250 and 250 W respectively at standard conditions. A tilt of 30^o is considered. The heat production per m^2 of the collector (P_{th}) is given by Eq. (1).

$$P_{th} = P_{th,exp} - P_{th,loss} \tag{1}$$

where $P_{th,exp}$ is the exploitable thermal power and $P_{th,loss}$ is the thermal loss of the collector given by suitable equation which takes into consideration thermal loss characteristics of the PVT panels.

According to the manufacturer, the exploitable thermal power per m^2 is given by Eq. (2).

$$P_{th,exp} = n_{th,b} \cdot I_{b,T} \cdot IAM_{th} + n_{th,d} \cdot (I_{d,T} + I_{refl,T}) \tag{2}$$

where $I_{b,T}$, $I_{d,T}$, $I_{ref,T}$ are the hourly beam, diffuse and reflective radiation components on the tilted collector surface, $n_{th,b}$ and $n_{th,d}$ are the thermal efficiency coefficients that correspond to heat acquisition by beam and diffuse radiations respectively, and IAM_{th} is the thermal incidence angle modifier.

The electrical production per m^2 of the collector is given by Eq. (3).

$$P_{el} = \left[n_{el,b} \cdot \left(I_{b,T}\right) \cdot IAM_{el} + n_{el,d} \cdot \left(I_{d,T} + I_{refl,T}\right)\right] \cdot [1 - a_{el}(T_m - T_{stc})] \tag{3}$$

where T_{stc} is the temperature at standard test conditions equal to 25 ^oC, $n_{el,b}$ and $n_{el,d}$ are the electrical efficiency coefficients that correspond to electrical production by beam and diffuse radiation components, a_{el} is the temperature loss coefficient, and IAM_{el} is the electrical incidence angle modifier.

Further details of the collector with its performance parameters and modelling features are provided by Bernando et al., 2013 and Gomes et al., 2014.

3.4 Water tanks

The system model is supplemented with two different types of water tanks (see Fig. 1): main water tank and buffer water tank. The main water tank is supplied with heat directly from the PVT collectors at elevated temperature for producing hot water. In case this is not enough, the heat pump delivers the remaining heat to this tank. Stratification is needed to store as much as thermal energy while having high temperature differences in the inlet/outlet water flows (Rahman et al., 2016). Moreover, the mains water inlet has a very low temperature, favoring the stratified temperature distribution. Thus, an immersed heat exchanger is included, in which the tap water is circulated. The main water tank is modeled by splitting the tank in a finite number of 1-D volumes across the axis of equal height (Panaras et al., 2013) and applying energy balance in each volume. Heat transfer occurs between the volumes and between the volumes and the immersed heat exchanger. Ambient heat losses are calculated from each volume separately, according to its temperature and surface in contact with the tank walls.

There are two buffer tanks with their main functions as follows:

1. The solar buffer tank for storing the low-temperature heat produced by the collectors for supplying the

heat pump.

2. The space buffer tank for storing hot/chilled water for supplying the building's space heating/cooling network during the winter/summer season respectively, connected to the condenser/evaporator of the heat pump.

The modeling approach of the above two tanks is simple, since their temperature range is limited, usually by about ±10 °C, with a small variation between the inlet/outlet temperature of the water flows. This makes it possible to model these tanks as a single-volume tank, assuming the same water temperature within the whole tank (Panaras et al., 2013). This temperature is calculated based on the heat source and sink, as well as on the heat losses to the ambient through an unsteady energy balance equation.

3.5 Heating and cooling demand profiles

The complete system model considers a typical heating and cooling demand of a multi-family residential building. Heating includes both space heating and DHW. The space heating and cooling demand profile is estimated by an in-house code developed in Python exclusively for that purpose. The aforementioned calculations are based on thermal zones (one for each floor), thermostat preferences, building specifications (e.g. surface area and U values of the walls), solar heat gains and internal gains from occupants, according to Hoogsteen et al., 2016 and ASHRAE Handbook, 2017. A smart thermostat approach is introduced into the code, for restricting the sharp increase of space heating and cooling demand at peak hours, and thus smooth the profiles, indicating a realistic handling of the building loads. Furthermore, it is considered that the temperature in each floor is stabilized to a certain value, when occupants are absent. Calculation of the necessary thermal loads to keep the indoor air temperature to the set-point temperature, allowing a variation of ±1 K, is based on distinguishing between heating and cooling seasons. The necessary weather data to perform the calculations are the annual solar irradiation components and ambient temperature, with the former obtained from TRNSYS software (Klein et al., 2005).

A small multi-family building with five 100-m^2 well-insulated apartments is considered. Moreover, each apartment occupies a whole floor and hosts a family composed of two adults and two children. The weather data of Athens, Greece, are used for the calculations with a time-step of 10 minutes.

A typical daily space heating and cooling profile is shown in Fig. 2 during a winter (1st of January) and a summer day (1st of July) respectively, together with the internal heat gain that also includes the solar gain. The peak of the heat gain is higher during winter, since a larger amount of solar radiation reaches the glazing of the building.

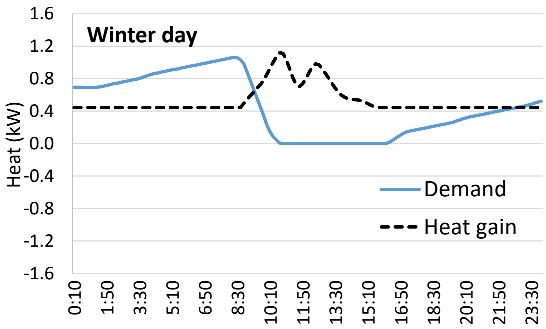

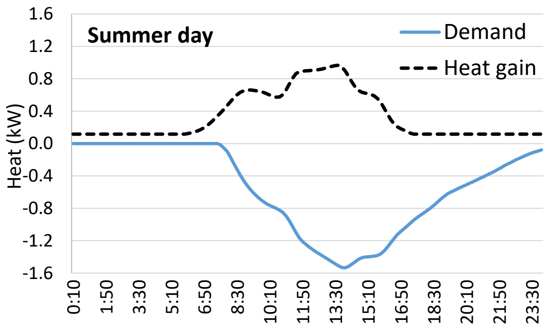

Fig. 2: Space heating and cooling demand and heat gain profile of each apartment during a winter day (left) and a summer day (right) in Athens, Greece

The specific energy demand of this building is about 100 kWh/m^2, divided into 59.45 kWh/m^2 for space heating and 40.34 kWh/m^2 for space cooling.

The DHW profile required by the model is calculated according to EN16147:2017 standard for water-heaters, hot water storage appliances and water heating systems (EU Regulation No 814/2013). The standard defines a 24-h measurement tapping cycle with its total thermal energy content of almost 12 kWh per apartment and per day, corresponding to the "L" profile. This profile is shown in Fig. 3, with the same used for all days of the year.

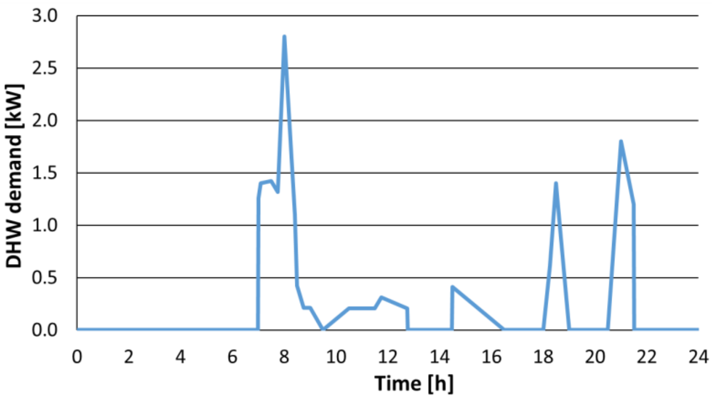

Fig. 3: DHW profile ("L") during the day, according to the standard EN16147:2017

This profile is included in the EES code, and in combination with the heating and cooling needs define the overall demand for the building energy system simulation.

4. Results and discussion

The main results are related to the energy production potential and the temporal performance of the main components. Since the PVT surface has an important role on the system performance, mostly for heating, its effect will be also examined. The results are initially presented for the reference case with a PVT surface of 50 m^2 for a residential building with 5 apartments for a typical day in January (winter) and July (summer) in Athens, Greece.

4.1 Winter day

The heat pump configuration is flexible, allowing the simultaneous operation of both compressors for the production for both space heating and DHW. This is clearly depicted in Fig. 4 during the winter day.

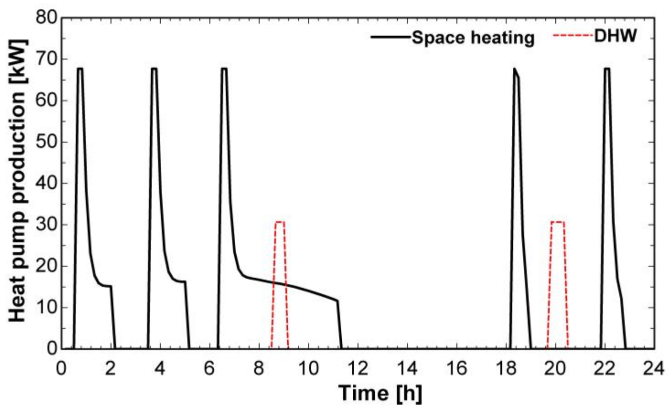

Fig. 4: Heat pump production for space heating and DHW during the winter day

The volume of the space heating buffer tank is 2 m^3, which is large enough to avoid the frequent switch-on of the heat pump. During this typical winter day, the heat pump operates five times for space heating production, mostly during the night and early in the morning, to increase the temperature of the space buffer tank to 45 ^{o}C. On the other hand, the production of 30 kW for DHW is needed only twice per day for charging the main water tank, closely following the demand profile of Fig. 3.

The charging process is shown in Fig. 5 through the average temperature of the stored water in all three tanks (main, space heating buffer, and solar buffer). The average temperature of the main tank is divided into the temperature of its upper part (heat supplied by the heat pump) and to its lower part (heat supplied by the PVT collectors).

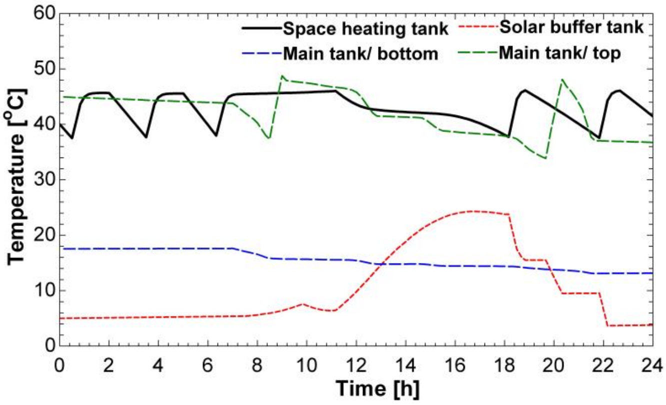

Fig. 5: Average temperature of the water tanks (main tank divided into top and bottom parts) during the winter day

The temperature of the space heating buffer tank ranges between 40 and 45 °C, with the lower limit defined as the minimum to engage the heat pump operation. From 11:30 to 18:00 all space heating demand is covered by the stored thermal energy of the water, gradually reducing its temperature, without the need to operate the heat pump during this period.

The water of the main tank at the top part is kept at elevated temperature the whole day, showing some fluctuations, according to the DHW demand and the heat pump operation. The bottom part remains at a low temperature, since the PVT collectors supply a very small amount of heat to the main tank during this day. The rest is directed to the solar buffer tank, with its temperature always kept within the range of 5-25 °C. When the minimum threshold of 5 °C is reached, the heat pump switches its heat source to the ambient air. Moreover, the water temperature in this tank reaches 25 °C late in the afternoon, after being charged during the whole day, allowing for a very efficient heat pump operation, as shown in Fig. 6, in which the COP is presented along with the electricity consumption of the heat pump.

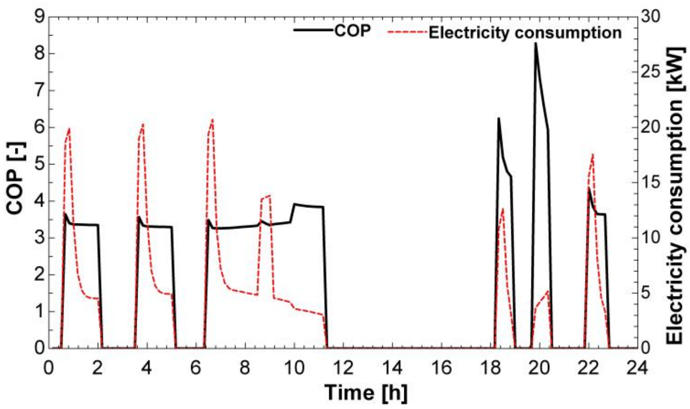

Fig. 6: COP and electricity consumption of the heat pump during the winter day

The COP is in the range of 3.5-4 from midnight until noon, but increases significantly in the evening to 5-6 due to the elevated solar buffer tank temperature at the same period (see Fig. 5). As a result, the demand for electricity is reduced to values below 17 kW between 18:00 and 23:00, whereas between 00:00 and 11:00 is up to 20 kW.

4.2 Summer day

During summer, the space buffer tank (see Fig. 1) is used to store chilled water. Heat is extracted from this tank to keep it at a low temperature, with the lowest limit set to 7 °C, which is the standard for space cooling appliances with water (e.g. fan coils). Figure 7 shows the heat pump operation to reduce the temperature of this tank, as well as to charge the main tank for covering the DHW loads for a typical summer day. Simultaneous operation at these two modes is not possible, as described previously.

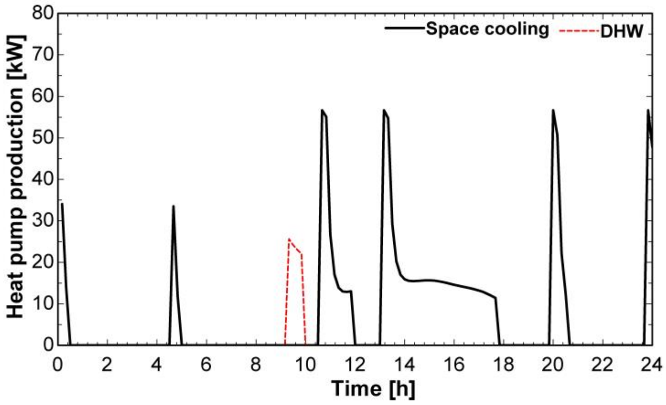

Fig. 7: Heat pump production for space cooling and DHW during the summer day

The heat pump operates five times during the summer day, with a long operation during noon and afternoon, when cooling loads of the building are higher (see Fig. 2). During start-up, the maximum cooling capacity of about 55 kW is observed due to the high temperature difference (inlet/outlet) of the water at the condenser side. Moreover, the largest fraction of DHW demand is directly supplied by the PVT collectors, heating up the main water tank (its bottom part). This results to the operation of the heat pump for DHW production only once during this day with a duration of about 50 minutes. The evolution of the water tank temperatures as the result of the charging by the heat pump is shown in Fig. 8.

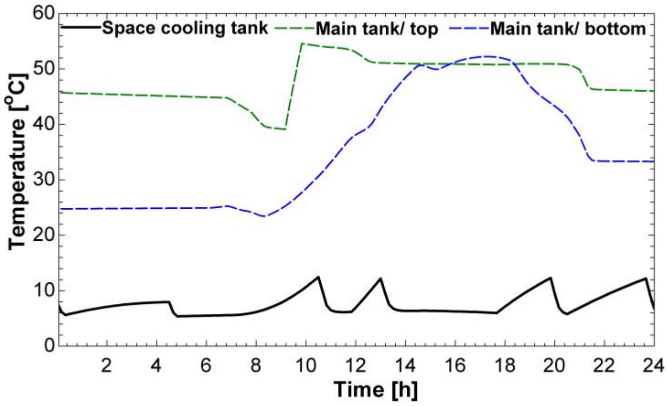

Fig. 8: Average temperature of the water tanks (main tank divided into top and bottom parts) during the summer day

The heat pump starts operating, when the temperature of the space cooling buffer tank approaches the upper 12 °C threshold, which takes place at around noon, due to the high cooling loads. In this mode, the heat sink at the condenser side of the heat pump is the ambient air.

Moreover, the water temperature at the main tank is mostly charged by the PVT collectors, since its temperature at the bottom part is adequate for heating the mains water for most of the hours during the summer day. The heat pump operates for DHW production only early in the morning, when the PVT heat production is very small and not adequate to ensure a high enough temperature for the DHW flow. The result is the rapid increase of the average water temperature at the upper part of the main tank to over 50 °C, which is kept at such temperature level until the evening.

The heat pump for DHW production operates with a high COP in the range of 6-7, since it is supplied with the heat of the ambient air, whose temperature is about 30 °C at noon. This is shown in Fig. 9, together with the electricity consumption for both DHW and space cooling production.

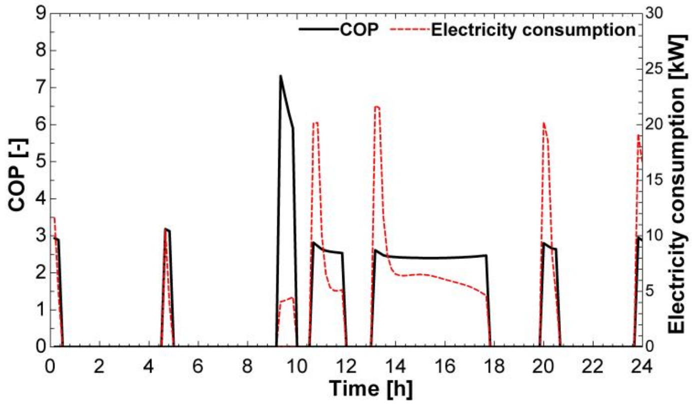

Fig. 9: COP and electricity consumption of the heat pump during the summer day

The COP for space cooling production is always kept in the range of 2.7-3.1 during the summer day. The COP for cooling is reduced during the noon-afternoon hours, when the ambient temperature shows the maximum values during the day, whereas early in the morning the performance is improved, reaching a COP of 3.1 and an electricity consumption of 10 kW.

4.3 Comparison of winter and summer system operation

The main performance indicators are presented in Table 1 during the winter and summer day. These indicators are related to both the heat pump and the PVT collectors and they are averaged during the two days.

Table 1: Performance indicators during the winter and summer day

Indicator (daily averaged)	Winter day	Summer day
COP for space heating (-)	3.66	-
COP for DHW (-)	4.25	6.61
COP for space cooling (-)	-	2.84
Space heating production (kWh)	313.6	-
DHW production by the heat pump (kWh)	47.07	18.29
Space cooling production (kWh)	-	149.2
Heat pump electricity consumption (kWh)	76.73	55.73
PVT electricity efficiency (%)	5.52	4.57
PVT thermal efficiency (%)	35.18	21.61
PVT electricity production (kWh)	7.96	16.33
PVT heat production (kWh)	50.75	77.21

The heat pump operates with a higher COP for DHW production by 55%, during summer, since its heat source has an elevated temperature during this period, which enhances its performance. On the other hand, the COP for space cooling is similar to standard heat pumps, since the unit relies on ambient air for rejecting the condenser heat. Moreover, the PVT collectors show a higher electrical and thermal efficiency during winter, due to the reduced working temperatures, which is beneficial for their performance. This is more pronounced for the thermal efficiency, which is increased by 63% compared to the operation during the summer day, while the electrical efficiency is less sensitive to the water temperature of the collectors.

4.4 Annual system performance

The annual system performance has been also examined, with the average COP of the heat pump during each month of the year shown in Fig. 10.

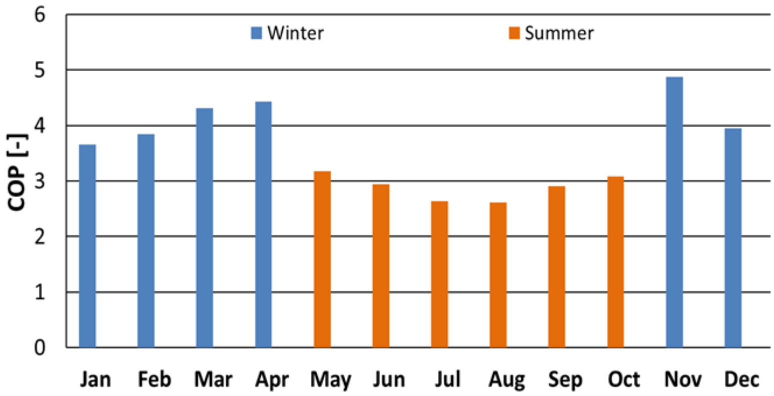

Fig. 10: Average COP of the heat pump during each month

The average COP for heating is lower than 4 during the winter months (December to February), while it is increased over 4 in spring and autumn, as a direct result of higher ambient temperature and availability of solar radiation. During the cooling period, when the space cooling production from the heat pump is much higher than the DHW production, the COP shows its lowest values during July and August, which are the hottest months of the year, while it increases to about 3 during May and October.

The results of a similar analysis concerning the electrical and thermal efficiency of the PVT collectors during each month are presented in Fig. 11.

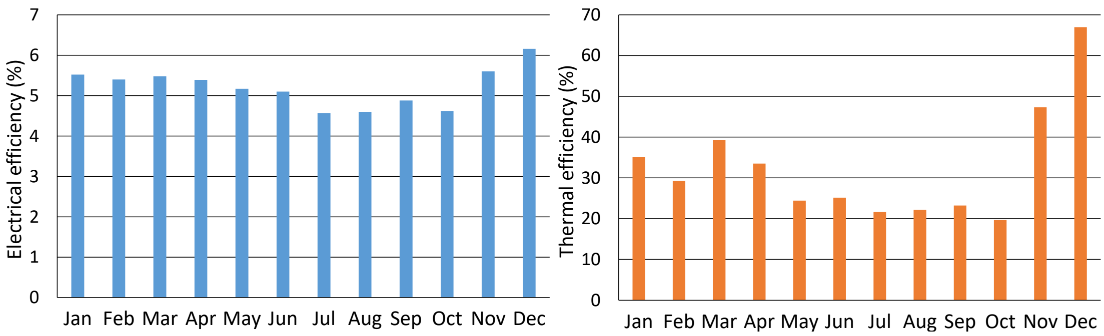

Fig. 11: Electrical (left) and thermal efficiency (right) of the PVT collectors during each month

Both electrical and thermal efficiency are increased during the winter period, when the PVT collectors operate for charging the solar buffer tank, with their temperature always kept below 25-30 ºC. The highest performance is observed in December with an electrical efficiency exceeding 6%, while the average is about 5%. The highest thermal efficiency of the PVT collectors of 46% is also reached during this month, since the ambient temperature is still not very low with many moments producing heat at low temperature for supplying the solar buffer tank. Both these aspects favor the performance of the PVT collectors.

4.5 Effect of the PVT surface

The final part of this work examines the effect of the PVT surface on the overall system performance. The case presented previously relies on a PVT surface of 50 m^2 and reaches a maximum water temperature of 70 ºC in the main tank during summer. Therefore, it is possible to increase the PVT surface to even 100 m^2 and still avoid over-heating, reaching a maximum tank temperature of 95 ºC. By doing so, the system performance is improved mostly during winter with a higher heat production, with a positive impact on the COP of the heat pump. Moreover, the electricity production of the collectors is increased, but still the electricity consumption of the heat pump is always higher, and thus defining the net electricity consumption at system-level, which provides their difference.

The annually averaged performance indicators of the examined system are presented in Table 2 for a variable PVT collectors' surface.

Table 2: Performance indicators for different PVT collectors' surfaces

Indicator (annually averaged)	PVT collectors' surface (m^2)		
	20	**50**	**100**
COP for space heating (-)	4.03	4.13	4.21
COP for DHW (-)	5.70	5.75	5.77
COP for space cooling (-)	2.89		
Net electricity consumption (MWh)	16.44	13.65	9.53
PVT electrical efficiency (%)	5.36	5.20	5.03
PVT thermal efficiency (%)	37.99	31.77	24.63

The increase of the PVT surface from 20 m^2 to 100 m^2 improves the COP for space heating by 5%, while the COP for DHW shows a minor increase and remains practically the same. During summer, the heat pump uses only ambient air for cooling production, which does not depend on the PVT surface and therefore it is exactly the same. Finally, the efficiency of the PVT collectors is reduced, when a larger surface is used, due to the higher working temperatures, and this is especially obvious on the thermal efficiency, which reduces even below 25% in case a 100 m^2 PVT surface is used.

5. Conclusions

A flexible solar-based system for heating and cooling is proposed, with the dual-source heat pump being capable to select the source that maximizes its performance. The system performance greatly increases with the use of the PVT collectors that operate with a higher electric and thermal efficiency especially during winter, when their high-temperature operation is avoided.

During winter, the exploitation of the low-temperature heat produced by the PVT collectors allows the heat pump to operate with a high COP for both space heating and DHW production, and at the same time the PVT efficiency reaches higher values. On the other hand during summer, the solar-assistance mode of the heat pump introduces a minor improvement, only for DHW production, since the cooling demand is much higher than the DHW needs, for the weather data of Athens, Greece.

The next steps of this work are to conduct tests on an improved version of the PVT collector and on the flexible heat pump, and examine the system performance under a larger range of scenarios and cases, such as for other locations in Europe (e.g. with higher heating and no cooling needs), and for different building types including buildings without DHW needs (e.g. office buildings). Finally, a significant improvement of the system configuration will be the addition of a ground heat exchanger (e.g. borehole thermal energy storage) as an additional potential heat source for the heat pump, resulting to a multi-source configuration, expected to offer significant performance improvement for cooling production during summer.

6. Acknowledgments

This work has been performed within the RES4BUILD project (Renewables for clean energy buildings in a future power system) – Horizon 2020 program, Grant Agreement no. 814865.

7. References

ASHRAE, ASHRAE Handbook, 2017. Fundamentals. SI edition. Ashrae, USA.

Bernardo, R., et al., 2013. Measurements of the electrical incidence angle modifiers of an asymmetrical photovoltaic/thermal compound parabolic concentrating-collector. Engineering, 5(01), p.37.

Buker, M.S. and Riffat, S.B., 2016. Solar assisted heat pump systems for low temperature water heating applications: A systematic review. Renewable and Sustainable Energy Reviews, 55, pp.399-413.

EU Regulation No 814/2013 of 2 August 2013 implementing Directive 2009/125/EC of the European

Parliament and of the Council with regard to ecodesign requirements for water heaters and hot water storage tanks; https://eur-lex.europa.eu/eli/reg/2013/814/2017-01-09 (accessed on 16/07/2020).

Fine, J.P., Friedman, J. and Dworkin, S.B., 2017. Detailed modeling of a novel photovoltaic thermal cascade heat pump domestic water heating system. Renewable Energy, 101, pp.500-513.

Gomes, J., Diwan, L., Bernardo, R. and Karlsson, B., 2014. Minimizing the impact of shading at oblique solar angles in a fully enclosed asymmetric concentrating PVT collector. In Energy Procedia (Vol. 57, pp. 2176-2185).

Guo, X. and Goumba, A.P., 2018. Air source heat pump for domestic hot water supply: Performance comparison between individual and building scale installations. Energy, 164, pp.794-802.

Hoogsteen, G., Molderink, A., Hurink, J.L. and Smit, G.J., 2016, April. Generation of flexible domestic load profiles to evaluate demand side management approaches. In 2016 IEEE International Energy Conference (ENERGYCON) (pp. 1-6). IEEE.

Kim, T., Choi, B.I., Han, Y.S. and Do, K.H., 2018. A comparative investigation of solar-assisted heat pumps with solar thermal collectors for a hot water supply system. Energy Conversion and Management, 172, pp.472-484.

Klein, S.A. et al., 2005. TRNSYS 16: A Transient System Simulation Program, Solar Energy Laboratory, University of Wisconsin, Madison, USA, http://sel.me.wisc.edu/trnsys.

Klein, S.A., 2020. Engineering Equation Solver-EES, Version 10.834, Academic Professional.

Kosmadakis, G. and Neofytou, P., 2019. Investigating the effect of nanorefrigerants on a heat pump performance and cost-effectiveness. Thermal Science and Engineering Progress, 13, p.100371.

Naranjo-Mendoza, C., Oyinlola, M.A., Wright, A.J. and Greenough, R.M., 2019. Experimental study of a domestic solar-assisted ground source heat pump with seasonal underground thermal energy storage through shallow boreholes. Applied Thermal Engineering, 162, p.114218.

Panaras, G., Mathioulakis, E. and Belessiotis, V., 2013. Investigation of the performance of a combined solar thermal heat pump hot water system. Solar Energy, 93, pp.169-182.

Rahman, A., Smith, A.D. and Fumo, N., 2016. Performance modeling and parametric study of a stratified water thermal storage tank. Applied Thermal Engineering, 100, pp.668-679.

Vaishak, S. and Bhale, P.V., 2019. Photovoltaic/thermal-solar assisted heat pump system: Current status and future prospects. Solar Energy, 189, pp.268-284.

Wang, X., Xia, L., Bales, C., Zhang, X., Copertaro, B., Pan, S. and Wu, J., 2020. A systematic review of recent air source heat pump (ASHP) systems assisted by solar thermal, photovoltaic and photovoltaic/thermal sources. Renewable Energy, 146, pp.2472-248.